Elicitation of Scattering Parameters of Dual-halo Dual-dielectric Triple-material Surrounding Gate (DH-DD-TM-SG) MOSFET for Microwave Frequency Applications

Neeraj GUPTA[1], *Prashant KUMAR*[2]

[1]Department of Electronics & Communication Engineering, Amity University Haryana, 122413 Haryana, Gurugram, India
[2]Department of Electronics & Communication Engineering, J.C. Bose University of Science & Technology, YMCA, Mathura road, Sector 6, 121006 Faridabad, India

neerajsingla007@gmail.com, pk.vlsi@gmail.com

DOI: 10.15598/aeee.v19i1.3788

Article history: Received Aug 25, 2020; Revised Nov 10, 2020; Accepted Jan 15, 2021; Published Mar 31, 2021.

Abstract. *This paper presents an analytical model for intrinsic short-circuit admittance (Y) parameters of DH-DD-TM-SG MOSFET. Y parameters have been modeled using different small-signal equivalent circuit parameter which is used to find the Scattering parameters. These Y parameters have further been employed for computing S-parameters. These parameters are further used to investigate the microwave performance parameters of the proposed device. The Unilateral Power Gain and the maximum oscillation frequency is determined to evaluatethe microwave performance. The proposed device shows a higher cut-off frequency (f_T) and maximum oscillation frequency as to TM-SG MOSFET. The proposed device exhibits a 4.2 % improvement in U_T, 2.81 % in G_{ms} and 6.9 % improvement in G_{MTPG} as compared to TMSG. The analytical result of DH-DD-TM-SG MOSFET is in accordance with the simulated results.*

Keywords

Admittance parameter, cut-off frequency, halo implantation, scattering parameter, triple material.

1. Introduction

The communication market has been drastically changing every year with the advancement in technology by developing improved radio frequency circuits. This required replacement of bulky and costly microwave devices with compact, low-power and economical devices. MOSFET is a better choice for wireless communication and microwave applications to enhance the Radio Frequency (RF) performance. But the performance of conventional MOSFET deteriorates due to the existence of inadmissible short channel effects during miniaturization [1] and [2]. The whole semiconductor industry is looking for an alternative device that can be further scaled aggressively. Multigate MOSFET is the best candidate for achieving the desired performance. It provides better controllability and scalability. The driving current provided by these advanced structures is very high. These structures show huge potential against SCEs. The cylindrical structure consists of large width even in the same occupied area which enhances the packaging density. Furthermore, the advancement in gate and oxide material has the advantage to make the device suitable for microwave applications.

The DH-DD-TM-SG MOSFET is a potential candidate for future generation devices whose performance remains at an acceptable level after scaling [3]. S-parameters are very common in microwave measurements. These parameters are used to find out the var-

ious imperative gains of a device. The appropriate method for analysing the MOSFET at high frequency is the estimation of the S-parameter [4] and [5].

The equivalent circuit model of the proposed device is presented. Y-parameters are extracted which further is used to calculate the S-parameter. The real and imaginary parts of the Y-parameter are considered for finding the S-parameter. The various microwave performance parameters are calculated. The Unilateral Power Gain, maximum stable gain, Stern stability factor and maximum transducer power gain have been investigated for the proposed device. The large value of various gain is desirable for maximum power transfer. The numerous gains are extracted using S-parameters. The analytical outcomes are well correlated with simulated outcomes which validate the model. The performance parameters are compared and the result reveals that DH-DD-TM-SG MOSFET has superior gain over their counterparts.

2. Analytical Model

The proposed device exhibits excellent control on the channel by the gates which allow continuous scaling. Figure 1 depicts the cross-sectional view of DH-DD-TM-SG MOSFET. In the Gate electrode, three materials are incorporated with different metal work functions which improve carrier transportation efficiency: The gate electrode with the work functions Φ_{M1} = 4.8 eV (Au), Φ_{M2} = 4.6 eV (Mo) and Φ_{M3} = 4.4 eV (Ti), respectively are used. The gate structure has been formed by considering Molybdenum (Mo) as gate material due to variation in N_2 implant changes its work function. Gate stack consists of two dielectric materials SiO_2 and HfO_2 which mitigate the leakage current. Halo doping improves the device behavior in terms of reduction in SCEs. The uniform doping profile is used with a doping concentration in halo and channel regions are 10^{24} and $10^{23}\cdot m^{-3}$, respectively. The resultant width is more in the case of surrounding gate MOSFET which enhances the packaging density [6] and [7].

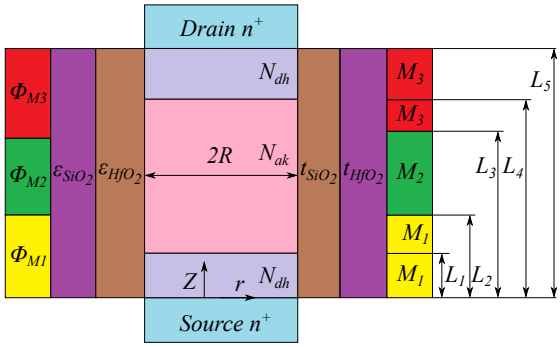

Fig. 1: A cross-sectional view of DH-DD-TM-SG MOSFET.

Figure 2 depicts the two-port equivalent circuit of the proposed device. The input port is corresponding to the gate-source terminal having voltage and current as V_i and I_i. The output port is represented by a drain-source terminal having voltage and current as V_o and I_o. Y-parameters are calculated using a small signal equivalent circuit [8] and [9]. A one-dimensional charge-control-based model is used to find out the intrinsic elements of the circuit. S-parameters are evaluated from Y-parameter to access the device performance in terms of maximum oscillation frequency and unilateral power gain.

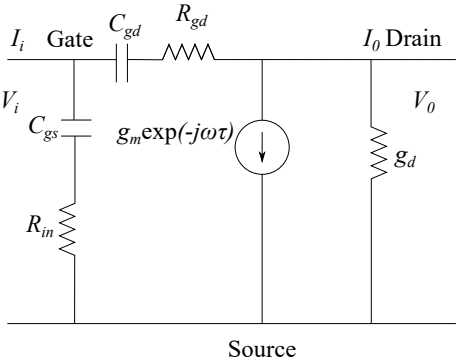

Fig. 2: Small signal equivalent circuit of DH-DD-TM-SG MOSFET.

Circuit theory is used to calculate the expression for admittance parameters.

- Input Admittance Y_{11}:

  Y_{11} is the ratio of the current to the voltage at the input port when $V_o = 0$.

$$Y_{11} = \left.\frac{I_i}{V_i}\right|_{V_o=0} = \frac{\omega^2 C_{gs}^2 R_{in}}{H_1} + \frac{\omega^2 C_{gd}^2 R_{gd}}{H_2} + j\omega\left(\frac{C_{gs}}{H_1} + \frac{C_{gd}}{H_2}\right), \quad (1)$$

  where $H_1 = 1+\omega^2 C_{gs}^2 R_{in}^2$ and $H_2 = 1+\omega^2 C_{gd}^2 R_{gd}^2$.

- Reverse Transfer Admittance Y_{12}:

  Y_{12} is the ratio of the input current to the output voltage when $V_i = 0$.

$$Y_{12} = \left.\frac{I_i}{V_o}\right|_{V_i=0} = -\frac{\omega^2 C_{gd}^2 R_{gd}}{H_2} - j\omega\left(\frac{C_{gs}}{H_1} + \frac{C_{gd}}{H_2}\right). \quad (2)$$

- Forward transfer Admittance Y_{21}:

  Y_{21} is the ratio of the output current to the input voltage when $V_o = 0$.

$$Y_{21} = \left.\frac{I_o}{V_i}\right|_{V_o=0} = \frac{g_m e^{-j\omega\tau}}{1 + j\omega C_{gs} R_{in}} - j\omega C_{gd}. \quad (3)$$

- Output Admittance Y_{22}:

  Y_{22} is the ratio of the output current to the output voltage when $V_i = 0$.

$$Y_{22} = \left.\frac{I_o}{V_o}\right|_{V_i=0} = g_d + \frac{\omega^2 C_{gd}^2 R_{gd}}{H_2} + j\omega\frac{C_{gd}}{H_2}. \quad (4)$$

The S-parameters are evaluated from Y-parameters using direct conversion which is given as:

S_{11} represents the input reflection coefficient. It is the ratio of the signal reflected to the incident at the input port with the output port truncated at Z_o. It is associated with matching of the input port to source impedance in the LNA design.

$$S_{11} = \frac{(1 - Z_o Y_{11})(1 + Z_o Y_{22}) + (Z_o^2 Y_{12} Y_{21})}{\Delta}. \quad (5)$$

S_{12} represents the reverse transmission coefficient. It is the ratio of the signal transmitted at the input to the signal incident at the output port with the input port truncated at Z_o. The feedback from output to the input of an amplifier is given by S_{12} which affects stability.

$$S_{12} = \frac{-2Z_o Y_{11}}{\Delta}. \quad (6)$$

S_{21} represents the forward transmission coefficient. It is the ratio of the signal transmitted at the output port to the signal incident at the input port with the output port truncated at Z_o. S_{21} is related to the maximum power gain of an amplifier. So, more value of S_{21} produces more gain and the device can be operated at a higher frequency range.

$$S_{21} = \frac{-2Z_o Y_{22}}{\Delta}. \quad (7)$$

S_{22} represents the output reflection coefficient. It is the ratio of the signal reflected to the incident at the output port with the input port truncated at Z_o. It is associated with matching of the output port to load impedance in the amplifier design.

$$S_{22} = \frac{(1 + Z_o Y_{11})(1 - Z_o Y_{22}) + (Z_o^2 Y_{12} Y_{21})}{\Delta}. \quad (8)$$

$$\Delta = (1 + Z_o Y_{11})(1 + Z_o Y_{22}) - Z_o^2 Y_{12} Y_{21}. \quad (9)$$

$Z_o = 50\ \Omega$.

A charge-based model is used to calculate C_{gs} and C_{gd} [10].

3. Results & Discussion

Figure 3 illustrates the change in overall gate capacitance, $C_{gg} = (C_{gs} + C_{gd})$ for DH-DD-TM-SG and TMSG MOSFET with the change in gate voltage. It can be noticed in the Fig. 3 that DH-DD-TM-SG MOSFET has a higher value of capacitance as compared to TMSG MOSFET. This is owing to the high dielectric constant present in the device. Furthermore, large carriers are available for current conduction due to halo doping. The device frequency does not deteriorate with an increase in capacitance in DH-DD-TM-SG MOSFET in comparison to TMSG MOSFET because of former has a higher value of transconductance. The frequency behavior of the device is mainly related to the capacitive nature of the device. The switching speed of a device is highly related to cut-off frequency (f_T) given as [11]:

$$f_t = \frac{g_m}{2\pi C_{gg}}. \quad (10)$$

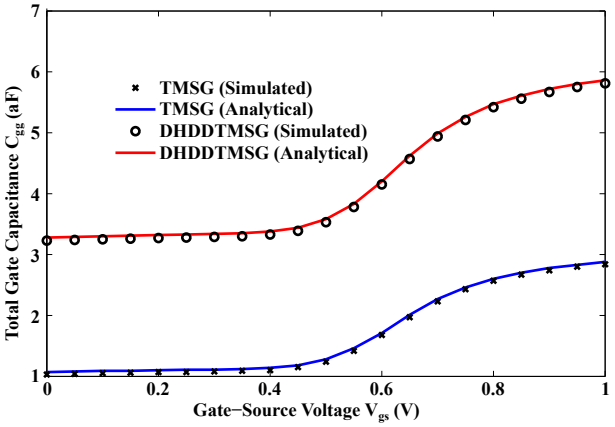

Fig. 3: Total Gate Capacitance versus Gate voltage for DH-DD-TM-SG and TM-SG MOSFET.

Figure 4 depicts and analyzes the S-parameters of the proposed device and TM-SG MOSFET with $t_{ox} = 2$ nm, $L = 30$ nm, $V_{gs} = 0.2$ V and $V_{ds} = 0.1$ V. The input and output reflection coefficients are represented by S_{11} and S_{22}. Ideally, the matching between two ports should be maximum with zero reflection coefficients. Figure 4(a) and Fig. 4(d) depict the variation in S_{11} and S_{22} with the change in frequency; S_{11} and S_{22} show a very small variation with the frequency.

As can be seen from the Fig. 4, the proposed structure exhibits a lower value of reflection coefficients than TM-SG MOSFET. S_{11} and S_{22} decrease with an increase in frequency. The existence of gate stack and triple metals at the gate enhances the gate control over the channel which improves the transconductance and current. Thus, diminishing the reflection coefficients and improving the matching between input and output ports.

Figure 4(b) and Fig. 4(c) highlight the variation in S_{12} and S_{21} with the change in frequency. The leakage factor from input to outport is represented by reverse transmission parameter S_{12}. It is also known

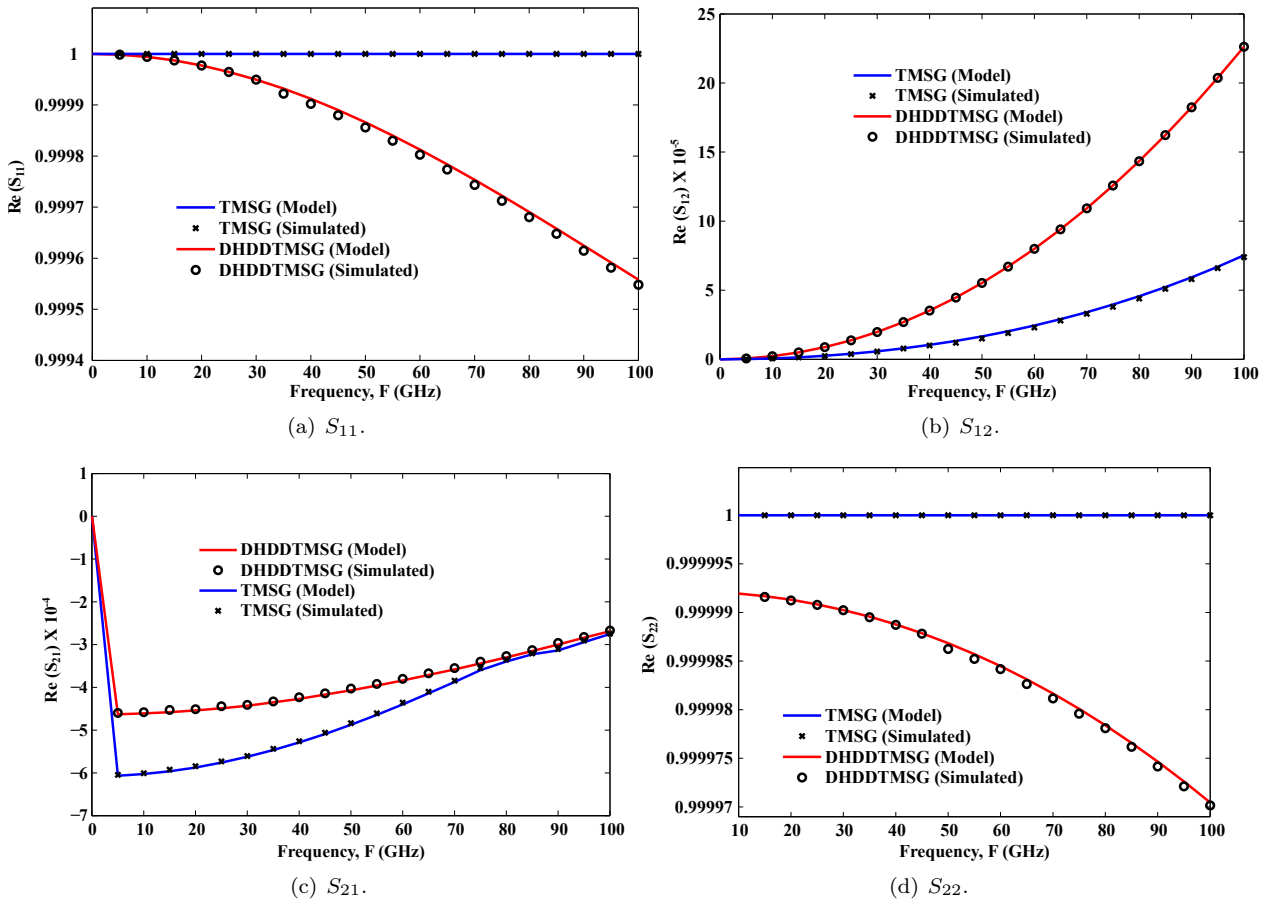

(a) S_{11}. (b) S_{12}.

(c) S_{21}. (d) S_{22}.

Fig. 4: S-parameter analysis of imaginary parts of DH-DD-TM-SG and TM-SG MOSFET.

as reverse voltage gain and its value should be higher because it contributes to the stability of a MOSFET. The signal power transferred from input to output port is known as forward voltage gain i.e. S_{21}. The larger value of S_{12} gives a larger gain of the device. The DH-DD-TM-SG MOSFET exhibits more value of S_{21} and S_{12} as to TM-SG MOSFET because of reduced SCEs and enhanced device performance.

Figure 5 illustrates the imaginary part of the S-parameter analysis. The imaginary parts of S_{11} and S_{22} exhibita lower value for the proposed device as compared to TM-SG due to better electrostatic control of the gate. The imaginary part of DH-DD-TM-SG MOSFET shows more value of S_{12} and S_{21} as to TM-SG MOSFET due to high current driving capability.

The power gain is a very imperative parameter for designing an amplifier for microwave applications. The two-port device is said to be active when U_T is more than 1 otherwise device is treated as passive. The maximum frequency of oscillation is the frequency at which the unilateral power gain becomes unity.

Figure 6 shows the U_T as a function of frequency at $L = 30$ nm. The U_T reduces exponentially with an increase in frequency as shown in Fig. 6. By further plotting the U_T curve, we obtained $f_{\max}$ as 850 GHz. The simulated results are in good agreement with the analytical results [12].

Figure 7 shows the maximum stable power gain with a change in frequency. This gain is extracted before the existence of instability in the device. With the significant increase in frequency, the maximum stable power gain decreases because of the reduction in the mismatch between two ports. The U_T exhibits an exponential decrease from the peak value of 36.7 dB to 12.17 dB for the proposed device and 33.24 dB to 5.19 dB for TM-SG MOSFET when frequency varies from 5 GHz to 100 GHz. There is a 4.2 % improvement in U_T as compared to TMSG and 5.1 % in comparison to a Dual Metal Gate (DMG) and 7.4 % in contrast to Double-Gate (DG) MOSFET.

The unilateral power gain and maximum stable gain is expressed using S-parameters. These gain parameters are essential for designing an amplifier at microwave frequencies. The simultaneous matching of two ports without any internal feedback gives the U_T. The Unilateral Power Gain in terms of the S-parameters is expressed as [13] and [14]:

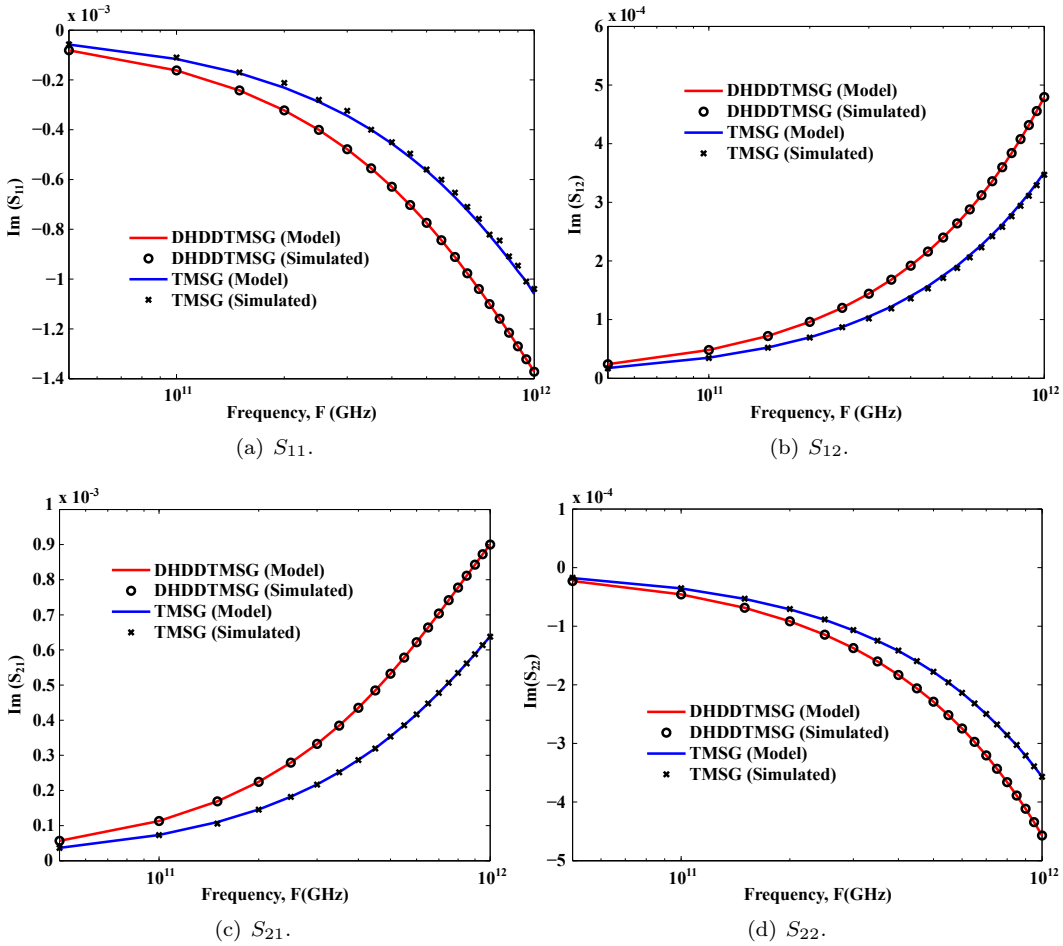

(a) S_{11}. (b) S_{12}.

(c) S_{21}. (d) S_{22}.

Fig. 5: S-parameter analysis of imaginary parts of DH-DD-TM-SG and TM-SG MOSFET.

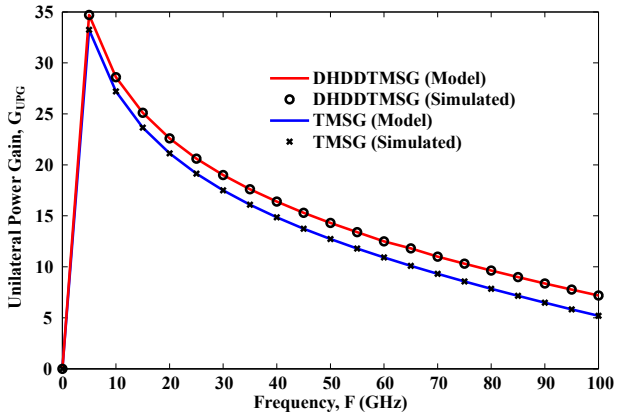

Fig. 6: Unilateral Power Gain with variation in Frequency.

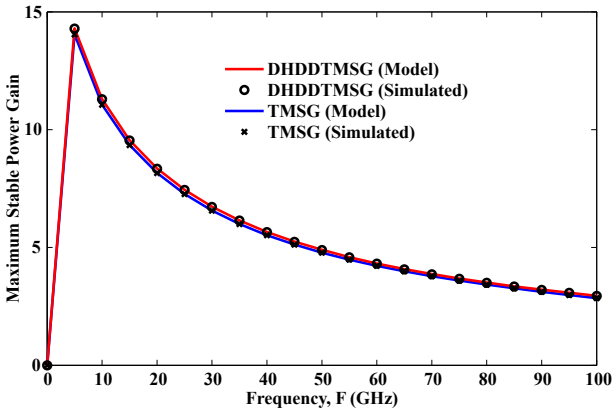

Fig. 7: Maximum Stable Power Gain with variation in Frequency.

$$U_T = \frac{\frac{1}{2}\left|\frac{S_{21}}{S_{12}} - 1\right|^2}{\theta\left|\frac{S_{21}}{S_{12}}\right| - Re\left|\frac{S_{21}}{S_{12}}\right|}, \tag{11}$$

$$\theta = \frac{1 - |\nabla|^2 - |S_{11}|^2 - |S_{22}|^2}{2|S_{12}S_{21}|}, \tag{12}$$

$$\nabla = S_{11}S_{22} - S_{12}S_{21}, \tag{13}$$

where θ is the stability factor. It is related to the stability factor and finds out the frequency to make the amplifier stable.

The reduction in G_{ms} with frequency takes place at a slower pace and the value is always more than 0 dB even for higher frequency. It implies better sta-

bility of the device which makes it appropriate for microwave applications. The resistive load in the network is considered to minimize the mismatch between two ports which gives G_{ms} when $\theta = 1$ [15] and [16].

$$G_{ms} = \frac{|S_{21}|}{|S_{12}|}, \tag{14}$$

Figure 7 depicts the deviation in G_{ms} with the change in frequency at $L = 30$ nm. It is the main parameter for designing a Low Noise Amplifier (LNA). The highest value of G_{ms} is 14.3 dB as observed from the figure. G_{ms} has a value above 0 dB at a higher frequency range which is mainly due to improved matching between two ports. There is a 2.81 % improvement in G_{ms} as compared to TMSG.

The stern stability factor is a measure of the absolute stability of the device. The stern stability factor is plotted up to the frequency of 100 GHz. The DH-DD-TM-SG MOSFET anticipates stern stability factor equal to unity as depicted in Fig. 8. It indicates a stable high-frequency behavior which makes it is suitable for an oscillator.

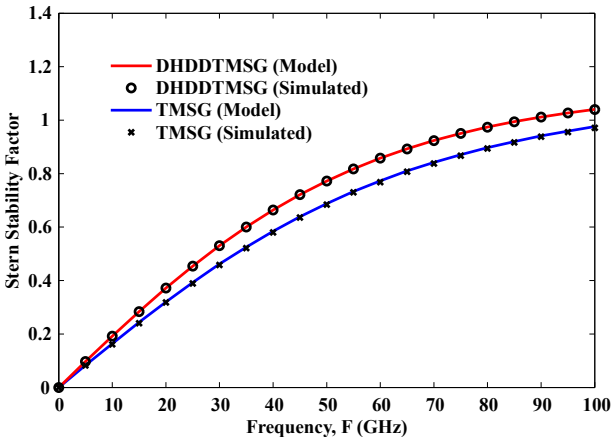

Fig. 8: Stern Stability Factor with variation in Frequency.

Figure 9 depictsthe change in G_{MTPG} with variation in frequency. The maximum gain which is achieved by an active port is G_{MTPG}. It is the highest gain among all other gains in microwave amplifiers and its value is also mentioned in the datasheet by the manufacturer. G_{MTPG} is given as:

$$G_{MTPG} = \frac{|S_{21}|^2}{(1-|S_{11}|^2)(1-|S_{22}|^2)}, \tag{15}$$

G_{MTPG} has a value above 0 dB at a higher frequency range which is mainly due to improved matching between input and output ports. There is a 6.9 % improvement in G_{MTPG} as compared to TMSG.

Figure 10 anticipates the fluctuation in current gain with frequency. G_I depends upon transconductance and gate-capacitances. There is a significant increase in transconductance for the proposed structure as compared to the existing MOSFET due to better gate control and enhanced carrier transport efficiency. Thus, G_I is higher for the proposed device in as to TM-SG MOSFET. There is a 3.2 % improvement in current gain as compared to TMSG. It is analyzed from different gains that the proposed structure reveals more gain as to TM-SG MOSFET owing to superior gate control. So, DH-DD-TM-SG MOSFET is a fruitful device for microwave applications.

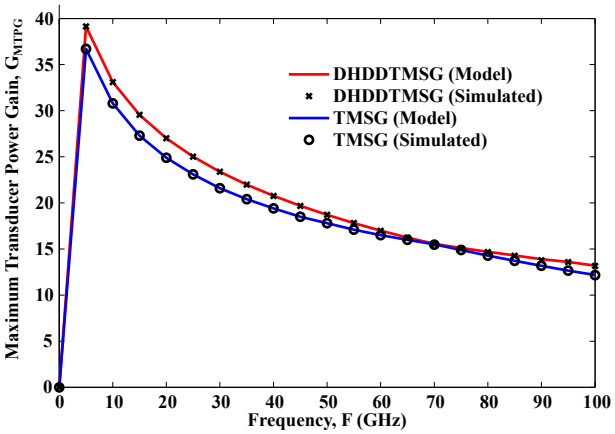

Fig. 9: Maximum Transducer Power Gain with variation in Frequency.

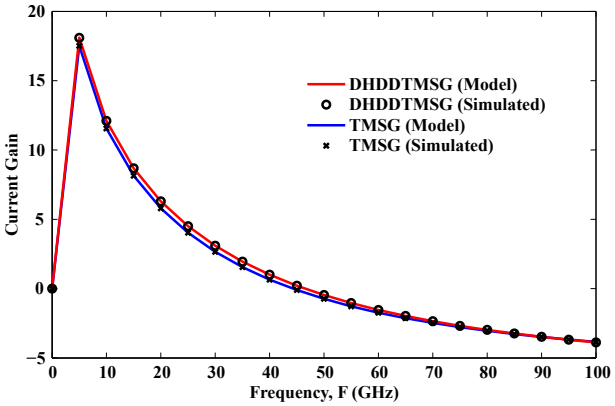

Fig. 10: Current Gain with variation in Frequency.

4. Conclusion

An intrinsic model for the proposed device has been presented in this paper. The scattering parameters are extracted from admittance parameters. The different gain parameters have been estimated. A DH-DD-TM-SG MOSFET exhibits mitigates in S_{11} and S_{22} and enhancement in S_{12} and S_{21} which makes it suitable for RF amplifiers. The results were compared with the TM-SG MOSFET. It has been noticed that DH-DD-TM-SG MOSFET shows better performance than

their counterparts MOSFET due to better gate control. The proper design of the device makes it suitable for high-frequency applications. The results indicate superior performance in the microwave range by the DH-DD-TM-SG MOSFET in terms of gains and scattering parameters.

Author Contributions

The idea of the research was conceptualized by N.G. N.G. also carried out the analytical modelling and simulation of Dual-Halo Dual-Dielectric Triple Material Surrounding Gate (DH-DD-TM-SG) MOSFET. The formal analysis and resources for the research was arranged by P.K. N.G. also prepared the original draft of the paper and P.K. did the review, proof reading and necessary editing in the article. Both the authors read and approved the final paper.

References

[1] RAY, R., R. DAS and M. CHANDA. Effect of fringing field capacitances in RF and small signal parameters of surrounding gate MOSFET. *Microsystem Technologies*. 2020, vol. 1, iss. 1, pp. 1–9. ISSN 1432-1858. DOI: 10.1007/s00542-020-04765-1.

[2] KUMAR, A., M. M. TRIPATHI and R. CHAUJAR. In_2O_5Sn based transparent gate recessed channel MOSFET: RF small-signal model for microwave applications. *AEU-International Journal of Electronics and Communications*. 2018, vol. 93, iss. 1, pp. 233–241. ISSN 1434-8411. DOI: 10.1016/j.aeue.2018.06.014.

[3] GUPTA, N., J. K. B. PATEL and A. K. RAGHAV. Performance and a new 2-D analytical modeling of a dual-halo dual-dielectric triple-material surrounding-gate-all-around (DH-DD-TM-SGAA) MOSFET. *Journal of Engineering Science and Technology*. 2018, vol. 13, iss. 11, pp. 3619–3631. ISSN 1823-4690.

[4] GHOSH, P., S. HALDAR, R. S. GUPTA and M. GUPTA. An Accurate Small Signal Modeling of Cylindrical/Surrounded Gate MOSFET for High Frequency Applications. *JSTS: Journal of Semiconductor Technology and Science*. 2012, vol. 12, iss. 4, pp. 377–387. ISSN 2233-4866. DOI: 10.5573/JSTS.2012.12.4.377.

[5] GHOSH, P., S. HALDAR, R. S. GUPTA and M. GUPTA. An analytical drain current model for dual material engineered cylindrical/surrounded gate MOSFET. *Microelectronics Journal*. 2012, vol. 43, iss. 1, pp. 17–24. ISSN 0026-2692. DOI: 10.1016/j.mejo.2011.10.001.

[6] GUPTA, N., J. K. B. PATEL and A. K. RAGHAV. An Accurate 2D Analytical Model for Transconductance to Drain Current ratio (g_m/I_d) for a Dual Halo Dual Dielectric Triple Material Cylindrical Gate All Around MOSFETs. *International Journal of Engineering*. 2018, vol. 31, iss. 7, pp. 1038–1043. ISSN 1728-1431.

[7] GUPTA, N., J. K. B. PATEL and A. K. RAGHAV. Modeling and analysis of Threshold Voltage for Dual-Halo Dual-Dielectric Triple-Material Surrounding-Gate Metal-Oxide-Semiconductor Field-Effect Transistors. *International Journal of Pure and Applied Mathematics*. 2018, vol. 118, iss. 18, pp. 3759–3771. ISSN 1314-3395.

[8] REWARI, S., V. NATH, S. HALDAR, S. S. DESWAL and R. S. GUPTA. Dual metal (DM) Insulated Shallow Extension (ISE) Gate All Around (GAA) MOSFET to reduce gate induced drain leakages (GIDL) for improved analog performance. In: *2017 Devices for Integrated Circuit (DevIC)*. Kalyani: IEEE, 2017, pp. 401–406. ISBN 978-1-5090-4724-6. DOI: 10.1109/DEVIC.2017.8073979.

[9] REWARI, S., V. NATH, S. HALDAR, S. S. DESWAL and R. S. GUPTA. Improved analog and AC performance with increased noise immunity using nanotube junctionless field effect transistor (NJLFET). *Applied Physics A*. 2016, vol. 122, iss. 12, pp. 1–10. ISSN 1432-0630. DOI: 10.1007/s00339-016-0583-9.

[10] LIU, F., J. ZHANG, F. HE, F. LIU, L. ZHANG and M. CHAN. A charge-based compact model for predicting the current–voltage and capacitance–voltage characteristics of heavily doped cylindrical surrounding-gate MOSFETs. *Solid-State Electronics*. 2009, vol. 53, iss. 1, pp. 49–53. ISSN 0038-1101. DOI: 10.1016/j.sse.2008.09.016.

[11] CHEN, J.-W., M. THURAIRAJ and M. B. DAS. Optimization of gate-to-drain separation in submicron gate-length modulation doped FET's for maximum power gain performance. *IEEE Transactions on Electron Devices*. 1994, vol. 41, iss. 4, pp. 465–475. ISSN 1557-9646. DOI: 10.1109/16.278497.

[12] *ATLAS 3D DEVICE Simulator*. 1st ed. Santa Clara: SILVACO International, 2010.

[13] SAHU, C. and S. MAJUMDAR. RF parameter extraction and S-parameter analysis of junctionless

silicon nanowire transistor. In: *2019 2nd International Conference on Innovations in Electronics, Signal Processing and Communication (IESC)*. Shillong: IEEE, 2019, pp. 7–12. ISBN 978-1-7281-0744-8. DOI: 10.1109/IESPC.2019.8902348.

[14] PATI, S. K., K. KOLEY, A. DUTTA, N. MOHANKUMAR and C. K. SARKAR. A new approach to extracting the RF parameters of asymmetric DG MOSFETs with the NQS effect. *Journal of Semiconductors*. 2013, vol. 34, iss. 11, pp. 114002. ISSN 1674-4926. DOI: 10.1088/1674-4926/34/11/114002.

[15] GOSWAMI, A., M. GUPTA and R. S. GUPTA. Analysis of scattering parameters and thermal noise of a MOSFET for its microwave frequency applications. *Microwave and Optical Technology Letters*. 2001, vol. 31, iss. 2, pp. 97–105. ISSN 1098-2760. DOI: 10.1002/mop.1369.

[16] GOSWAMI, A., A. AGRAWAL, S. BOSE, S. HALDAR, M. GUPTA and R. S. GUPTA. Substrate-effect-dependent scattering parameter extraction of short-gate-length IGFET for microwave frequency applications. *Microwave and Optical Technology Letters*. 2000, vol. 24, iss. 5, pp. 341–348. DOI: 10.1002/(SICI)1098-2760(20000305)24:5<341::AID-MOP16>3.0.CO;2-5.

About Authors

Neeraj GUPTA was born in Karnal, India. He received his Ph.D. in Engineering from Amity University Haryana, India in 2019. His research interests include Very-Large-Scale Integration (VLSI) design, Embedded systems, Device modelling, and Low power devices.

Prashant KUMAR was born in Faridabad, India. He received his M.Tech. in VLSI Design & Embedded Systemfrom Guru Jambheswar University of Science & Technology, Hissar, India in 2008. He is currently pursuing a Ph.D. in Device Modelling from J. C. Bose University of Science & Technology, YMCA, Faridabad, India. His research interests include VLSI design, Device modeling and Low power devices.